Iron and slag

11

Line Korsholm Lauridsen, Maryam Alizadeh Zolbin & Thomas Birch

Introduction

Iron is made by reducing ores in a furnace to form a raw bloom, which can be split to assess quality, divided for ease of trade, or formed into a bar for use or trade. Evidence for iron production is almost entirely absent from Jutland during the Viking Age (Buchwald & Voss 1992). This might be due to poor preservation of archaeological remains, but it has been argued that the alternative is more plausible – that iron was probably being imported from neighbouring regions (Buchwald 2005, 294).

Bloom fragments and purification slags from Ribe dated to around AD 750 infer that iron production still took place in western Jutland at that time. Typically, bog iron from west of the Weichsel Ice Age's Main Stationary Line in Jutland is characterized by a high phosphorus content, and the finds from Ribe derive from some of the last active iron production sites from the period (Buchwald 2005, 295). Whilst other finds analysed from Viking-age Jutland in the eighth and ninth centuries still show a Danish signature in the chemical composition of their slag inclusions, there are many others whose chemistry is consistent with origins in Norway, southern Sweden, and Germany – for example, an anchor from Ribe made from Norwegian-sourced iron (Buchwald 2005, 296–316). Growing interest in the multi-material trade networks between southern Norway and western Jutland highlight that steatite (soapstone) vessels and reindeer antler, as well as iron, were imported to Jutland (Ashby, Coutu & Sindbæk 2015; Baug et al. 2019), revealing that iron was part of a much larger resource and trade network in Scandinavia (Rundberget 2015, 173). Characterizing and contextualizing the importation of iron (as well as the longevity of locally produced iron) have, therefore, become a focal part of research into Viking-age ferrous metallurgy. The resolution of the chronological phases from Ribe's past and current excavations provides a unique opportunity to undertake such investigations.

The first process of working the iron is known as primary smithing. Secondary smithing is the process of manufacturing, repairing, or upcycling iron to produce an object. Studies of the metallurgical residues from the 1970–1976 excavations confirmed ironworking took place at Ribe, both the refining of raw iron (primary) and secondary smithing (Madsen 2004). This is further attested by the array of utilitarian and everyday finds made of iron, including locks and keys, different tools, and even weapons (Ottaway 2004).

A total of 3,218 pieces of iron were recovered at SJM 3 Posthustorvet, along with 1,700 pieces of slag. The slag residues represent a total weight of just under 53 kg. The majority of the ironwork is in a bad state of preservation due to the sandy soil in western Jutland, but a portion of the finds were X-radiographed and inspected, allowing some to be identified. Sampling of 37 artefacts was conducted for further archaeometallurgical investigations. The selection focused mostly on nails (or similar, e.g. clench nails, elongated/rod fragments), to allow for a discussion of utilitarian iron based on a representative group. The material

was selected across different phases to investigate for any changes through time, yielding information on the types of iron being used and its potential sources.

Slag debris

The slag remains from SJM 3 Posthustorvet have been counted (1,700 pieces) and weighed (around 53 kg in total), as summarized in Tables 11.1–2 and organized by phase, with those broadly phased aligned to the most appropriate specific phases. Further examination is required to determine the morphology and characteristics of the slag residues to determine their typology and metallurgical relevance. It is assumed that these remains derive from metallurgical activity within SJM 3, which would most likely derive from small-scale smithing operations, crucible metallurgy, or other pyrotechnic craft activity (e.g. glassworking). It is likely that any low-density ('light') porous pieces are fuel ash slag that are not diagnostic of any particular process other than a hearth or intense pyrotechnology, where alkaline elements from the fuel ash combined with the surrounding context/soil (normally rich in silica) to produce a vesicular 'bubbly' textured slag; they generally appear glassy and vary greatly in colour.

Slag can be used as a proxy for activity at SJM 3 Posthustorvet; comparing the recorded frequency (Fig. 11.1) and weight (Fig. 11.2) by phases provides some interesting observations. There appear to be two peaks in activity: the first is around phases F9 and F10, and the second is around phase F15 and F16. The steady rise in activity (phase F4 onwards) leads to the peak centring on phases F9 and F10; this is followed by a steady decline until phase F13. These results confirm that slag formation was inconsistent, defining episodes of more intense activity. This activity can be characterized further by normalizing the frequency of slag to the total weight per phase, to provide a crude average weight per slag piece. The average slag weight based on specific phasing (Fig. 11.3) as well as the average weight of all slag pieces combined from specific and broad phasing (Fig. 11.4) show similar trends. They reveal a general trend in which the weight of slag pieces declines beginning around phase F4 and terminating around phase F14. This implies that earlier activity produced larger slag fragments, but these decreased in size during later phases. This might be for two reasons: 1) the difference in average slag weights implies different processes during original formation, or 2) the differences may be attributed to higher degrees of

Phase	Slag	Broad phase	Slag	Broad phase	Slag
F2	4				
F3	319				
F4	39	F4/F5	15		
F5	34	F2/F3/F4/F5		F5/F6	8
F6	43	F4/F5/F6	3		
F7	46				
F8	95				
F9	214	F8/F9/F10	3		
F10	147				
F11	111	F10/F11	73		
F12	106	F11/F12	4		
F13	44	F12/F13	4	F13/F14	36
F14	77	F12/F13/F14	3	F14/F15	
F15	79				
F16	121	F14/F16/F17	2	F16/F17	7
F17	16	F14/F15/F16/F17	8	F15/F17	11
F18	28				
N	11				
Total	1534		115		62

Table 11.1. *Frequency of slag finds assigned to specific phases (left) or assigned more broadly to several phases (middle and right). N = No phase.*

Phase	Grams	Broad phase	Grams	Broad phase	Grams
F2	4				
F3	5983				
F4	855	F4/F5	2107		
F5	1508	F2/F3/F4/F5	0	F5/F6	86
F6	2629	F4/F5/F6	145		
F7	2338				
F8	4013				
F9	4722	F8/F9/F10	1156		
F10	4841				
F11	4602	F10/F11	445		
F12	2688	F11/F12	138	F12/F13	52
F13	774	F10/F11/F12/F13	97	F13/F14	1256
F14	1190	F12/F13/F14	113	F14/F15	0
F15	1553	F13/F14/F15	0		
F16	5028	F14/F16/F17	498	F16/F17	721
F17	259	F14/F15/F16/F17	246	F15/F17	370
F18	2214				
N	87				
Total	45288		4945		2485

Table 11.2. *Weight of slag (g) finds assigned to specific phases (left) or assigned more broadly to several phases (middle and right). N = No phase.*

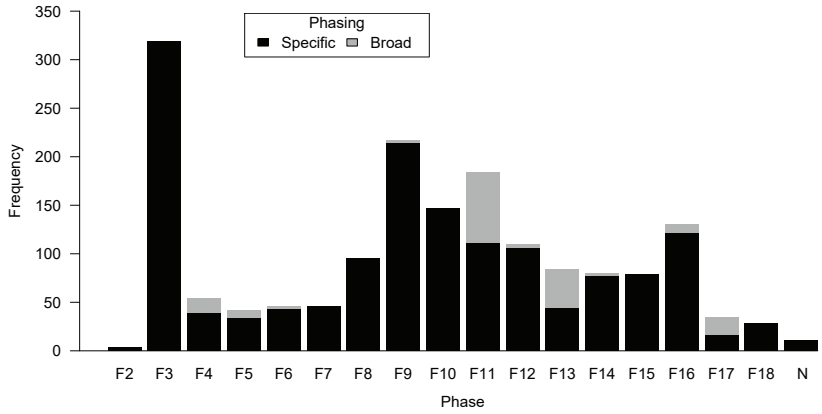

Figure 11.1. *Barplot of slag pieces per phase, highlighting those attributed to specific phases (black) and those more broadly phased (grey), assigned according to Table 1. N = Not phased.*

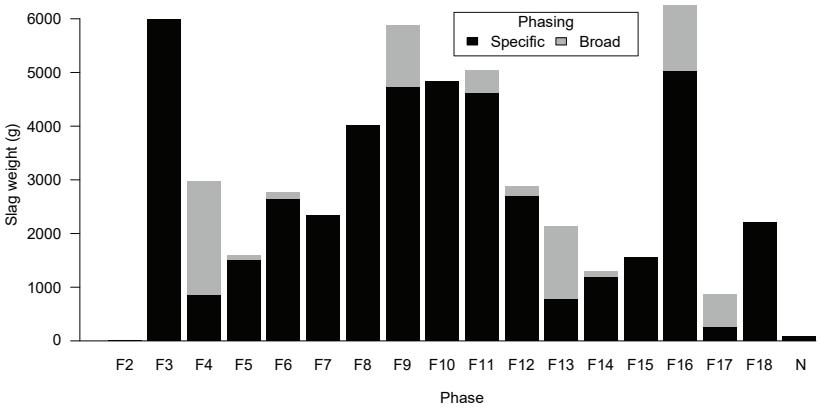

Figure 11.2. *Barplot of slag weight per phase, highlighting those attributed to specific phases (black) and those more broadly phased (grey), assigned according to Table 2. N = Not phased.*

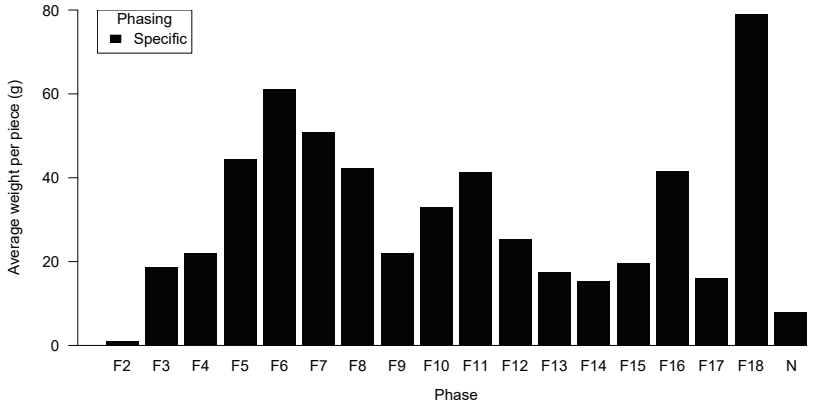

Figure 11.3. *Barplot of average slag weight per phase, showing only those that have been specifically phased (according to Table 1 and Table 2). N = Not phased.*

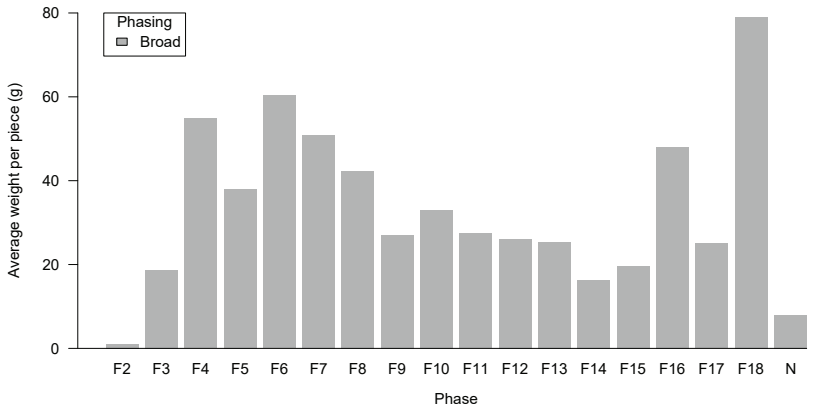

Figure 11.4. *Barplot of average slag weight per phase, combining those that have been specifically as well as broadly phased, according to the same assignments detailed in Table 1 and Table 2 (all slag pieces included). N = Not phased.*

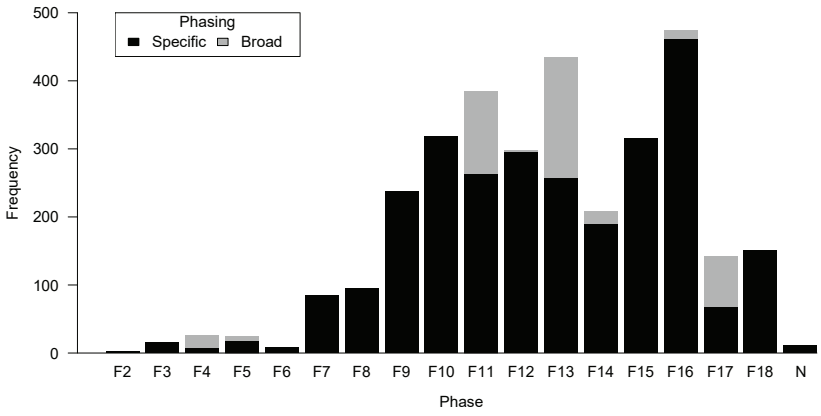

Figure 11.5. *Barplot of iron pieces per phase, highlighting those attributed to specific phases (black) and those more broadly phased (grey), assigned according to Table 3. N = Not phased.*

fragmentation of slag from the later phases. The declining average weight appears to support earlier work suggesting that more bloom refining took place during the earliest phases of settlement (Madsen 2004). Slags produced by bloom refining (primary smithing), like iron production slags, are much denser and larger than smithing residues produced by secondary smithing. The trend may be explained by a decrease in bloom refining, therefore implying a decreased reliance on locally produced iron.

The increase in likely smithing remains (represented by decreased average weight) coincides with increased secondary smithing activity. This is supported by an overall increase in iron finds (next section) during the same period (Fig. 11.5). The overall increase in iron finds (phases F7 to F16) is inversely related to an overall decrease in slag weight, suggesting a secondary smithing economy. The increase in iron finds recovered from SJM 3 Posthustorvet in the later phases may also be due to increased fragmentation, but the trend appears relatively clear. This may imply that iron was more predisposed to being retained at the immediate site, perhaps due to increased manufacture, repairs, and/or upcycling of retained material.

The increase in average slag weight and the number of iron finds leading up to phase F16 might infer the renewed emergence of purification slags and therefore the usage of local iron, though raw and partially refined blooms can travel great distances.

Phase	Iron	Broad phase	Iron	Broad phase	Iron
F2	2				
F3	16				
F4	6	F4/F5	20		
F5	17	F2/F3/F4/F5	1	F5/F6	7
F6	8	F4/F5/F6			
F7	84				
F8	95				
F9	238				
F10	318				
F11	263	F10/F11	122		
F12	294	F11/F12	4		
F13	256	F12/F13	16	F13/F14	162
F14	189	F12/F13/F14	18	F14/F15	1
F15	315				
F16	461	F14/F16/F17	1	F16/F17	12
F17	67	F14/F15/F16/F17	10	F15/F17	65
F18	150				
N	11				
Total	2790		192		247

Table 11.3. *Frequency of iron finds assigned to specific phases (left) or assigned more broadly to several phases (middle and right). N = No phase. The counts include indeterminable lumps and fragments and do not necessarily represent individual objects.*

Iron finds

A total of 3,218 iron finds were recovered from SJM 3 Posthustorvet, of which 2,779 pieces can be dated to specific phases (Table 11.3). Unfortunately, the preservation conditions of the iron are such that the majority present themselves as undiagnostic corroded lumps or unidentifiable fragments. Only the most well-preserved items were brought to Konserveringscenter Vest (Conservation in Ølgod) for X-radiography to assist in identification. A large number of items were discarded during this process, but all items were X-rayed and registered.

An initial assessment of the finds via visual examination as well as X-radiography enabled some finds to be identified (Table 11.4; Fig. 11.6 and 11.7). The vast majority are iron nails (142) and rivets (22). Other

Category	Amount
Nail	142
Rivet	22
Lump	22
Unidentified fragment	30
Bar/rod	8
Knife/knife fragment	7
Arrowhead	3
Firesteel	1
Ring	3
Fibula	1
Spurs	1
Key	1
Belt strap end (???)	2

Table 11.4. *Frequency of the diagnostic iron find categories identified from the SJM 3 excavations with the assistance of X-radiographs.*

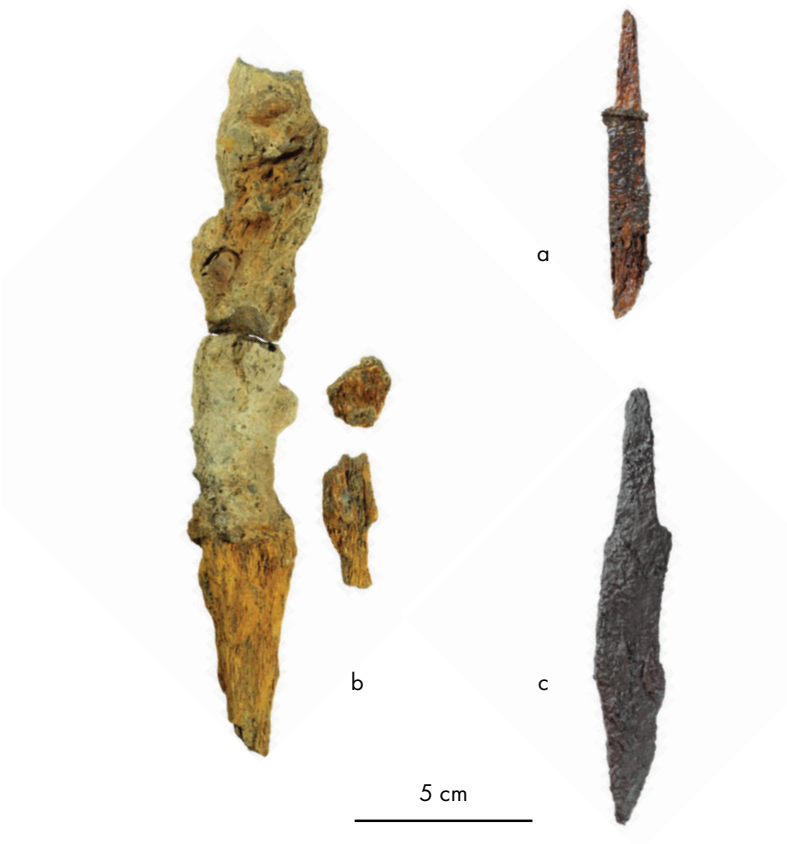

Figure 11.6. *Selected finds of knives, a) find no. A243 X542, ID 200304117; b) find no. A263 X515, ID 200300560; and c) find no. A316 X733 ID 200325062.*

identified artefacts include bars/rods (8), knives (7), arrowheads (3), and rings (3), as well as more unique finds (e.g. a firesteel, iron fibula, spurs, a key, and strap ends). These finds show a similar utilitarian character to previous work at Ribe (Ottaway 2004), although apparently in poorer condition and variety – for example, no apparent tools were evident. Some of these more exceptional finds, due to their rarity and/or shape, were kept for conservation.

An archaeometallurgical investigation of nails from SJM 3 Posthustorvet

Results from X-radiography were essential for aiding sampling of the artefacts selected, distinguishing the intact metal from corrosion. A magnetic inspection of this material complemented the visual assessment and X-radiography for determining areas deemed worth sampling within individual artefacts.

As nails represent the most prolific finds category for iron artefacts, it was decided to pursue this material for further investigation. A selection of 37 objects was made (Table 11.5), representing some 25% of the material deemed to be from the same or similar categories – nails (142) and bars/rods (8) – and representing just over 15% of the total iron remains listed in Table 11.4 (238). The selection is not only representative of the given finds category, but the material is representative of ironwork from SJM 3 Posthustorvet and derives from multiple phases, spanning phase F5 to phase F13. One sample (X1319) was determined to be mineral pyrite and was subsequently removed from analysis, resulting in a total of 36 samples for investigation.

Archaeometallurgical investigation of ironwork has the potential to yield information on smithing practices and technology, as well as potential sources of iron. The technical investigation set out to try and answer several important research questions:

- What type(s) of iron were used to manufacture nails, and did this change through time?
- What is the provenance of the iron used?
- Does the provenance of the iron highlight when the influx of Norwegian metal started, and how this trend persisted over time?

Figure 11.7. *a) Arrowheads, find nos A11 X361, ID 200304285 and A288 X675 ID 200304397; b) key, find no. A79 X76 ID 200304260; c) Fittings, find nos A335 X827, ID 200304196 and A230 X418, ID 200303994; d) Fire steel, find no. A331 X784, ID 200304166; e) Spur, find no. A148 X196, ID 200303820.*

Find no.	A Unit	Description	Phase	RX	ID
X1294	A882	Rod, fragmented	F5	Rx47	200304716
X1210	A590	Nail	F6	Rx47	200304712
X1319*	A871	*Mineral (pyrite)*	F6	Rx47	200304721
X1036	A440	Nail or clench nail	F7	Rx45	200304496
X1149-1	A590	Nail	F7	Rx46	200304704
X1149-2	A590	Nail	F7	Rx46	200304704
X1149-3	A590	Rod, fragmented	F7	Rx46	200304704
X1149-4	A590	Nail	F7	Rx46	200304704
X1149-5	A590	Fragment (plate?)	F7	Rx46	200304704
X1149-6	A590	Nail	F7	Rx46	200304704
X799	A335	Iron rod	F9	Rx37	200304175
X811	A335	Nail	F9	Rx37	200304181
X833	A350	Iron rod	F9	Rx38	200304238
X846	A354	Rod	F9	Rx34	200304015
X614-1	A263	Iron artefacts (nail etc.)	F10	Rx41	200304387
X614-2	A263	Rod	F10	Rx41	200304387
X614-3	A263	Rod	F10	Rx41	200304387
X614-4	A263	Nail	F10	Rx41	200304387
X632	A275	Nail	F10	Rx4	200304414
X640	A263	Folded iron rod	F10	Rx43	200304418
X163-2	A130	Cramp	F13	Rx23	200303757
X133-1	A114	Nail	F13	Rx18	200303715
X133-2	A114	Nail	F13	Rx18	200303715
X133-3	A114	Lump	F13	Rx18	200303715
X137	A114	Nail	F13	Rx18	200303719
X143-1	A114	Nail	F13	Rx19	200303724
X143-2	A114	Nail	F13	Rx19	200303724
X143-3	A114	Clench nail	F13	Rx19	200303724
X143-4	A114	Nail	F13	Rx19	200303724
X143-5	A114	Nail	F13	Rx19	200303724
X146-1	A114	Nail	F13	Rx19	200303726
X146-2	A114	Rod	F13	Rx19	200303726
X146-3	A114	Nail	F13	Rx19	200303726
X146-4	A114	Nail	F13	Rx19	200303726
X148	A114	Long pointy artefact	F13	Rx20	200303729
X163-1	A130	Little iron rod	F13	Rx23	200303757
X163-2	A130	Cramp	F13	Rx23	200303757
X167	A127	Iron	F13	Rx23	200303761

Table 11.5. *List of the artefacts selected for archaeometallurgical analysis from SJM 3 Posthustorvet. Note that X1319 was confirmed to be mineral pyrite and excluded from the results. Rx = X-radiograph Number.*

Sample preparation

The most well-preserved artefacts were photographed at Moesgaard Museum's photo lab prior to sampling. Samples were extracted from the selected iron artefacts by sawing. These were prepared as standard metallographic blocks, mounted and polished, at the School of Engineering (NAVITAS/Aarhus University). in preparation for microscopic examination and chemical analysis. Samples were mounted using a Struers CitoPress-1 (c. 180–200°C) using conductive, phenolic hot-mounting resin. The metallographic specimens were then ground and polished using a Struers TegraPol-15 using the settings made for steel (5 minutes per grinding/polishing step: MD Piano 220 using water as a lubricant, MD Largo using Diapro A/L as a lubricant, MD Dac using Diapro Dac as a lubricant, and finally MD Nap using Diapro Nap-B as a lubricant). Samples were rinsed using deionized water and then ethanol before being dried with hot air. The specimens were etched using standard nital (100 ml C_2H_6O, 10 ml HNO_3) to reveal their microstructures. Etching was between 40 and 50 seconds with checks at 15, 30, and 40 seconds. After etching, samples were rinsed again using deionized water and ethanol as outlined previously and were then ready for microscopic and chemical analysis.

Metallography

Each specimen was examined optically (after chemical analysis) using a metallurgical reflected-light microscope (Zeiss AX10, Observer A1m with magnifying 100x/0.8 HD, housed at the School of Engineering, NAVITAS/Aarhus University). Images of the microstructures observed were recorded as optical micrographs using the Zen software. The results are summarized in the catalogue appending this chapter, with detailed descriptions of individual samples.

A summary table of observed microstructures and features are provided in Table 11.6. No evidence of cold-working or carburization through case-hardening (the absorption of carbon through the surface to produce a steely surface layer) was observed. All samples show ferritic areas, as is to be expected. Weld lines observed in some artefacts illuminate aspects of nail-production technology worthy of further investigation to assess for standardized practices. At least two samples show evidence of rapid cooling (quenching) in the form of quick-cooled microstructures (i.e. martensite).

Find no.	Phase	Description	Pearlite	Weld lines	Ferrite	Phosphorous	Steel (low-C)	Steel (mid-C)	Steel (high-C)	Widmanstätten	Remarks
X1294	F5	Rod, fragmented	■		■		■				
X1210	F6	Nail	■	■	■	■	■			■	
X1319	F6	Mineral									Excluded (pyrite)
X1036	F7	Nail or clench nail	■	■	■				■	■	
X1149-1	F7	Nail	■		■			■			
X1149-2	F7	Nail	■		■		■				
X1149-3	F7	Rod, fragmented	■	■	□				■		
X1149-4	F7	Nail	■		■				■		Martensite/bainite?/quenched
X1149-5	F7	Fragment (plate?)	■		■				■		Elongated slags
X1149-6	F7	Nail	■		■				■		
X799	F9	Iron rod			■	■					
X811	F9	Nail	■		■			■			
X833	F9	Iron rod	■			■					
X846	F9	Rod	■		■			■	□		Folded?
X614-1	F10	Iron artefacts (nail etc.)	■		■				■		
X614-2	F10	Rod	■		■				■		
X614-3	F10	Rod	■		■			■		□	Martensite
X614-4	F10	Nail	■		■				■	■	
X632	F10	Nail	■	■	■				■	■	
X640	F10	Folded iron rod	■		■				■	■	Ultra-high-carbon steel
X133-1	F13	Nail	■		■		■				
X133-2	F13	Nail	■		■			■		■	
X133-3	F13	Lump	■	■	■	■					
X137	F13	Nail	■		■	□					
X143-1	F13	Nail	■	■	■		■				
X143-2	F13	Nail		■	■				■		Very high-carbon steel
X143-3	F13	Clench nail			■		■				Low carbon?
X143-4	F13	Nail	■						■		Ultra-high-carbon steel
X143-5	F13	Nail	■		■			■	■	■	
X146-1	F13	Nail			■	■		■			
X146-2	F13	Rod	■		■	■		■			
X146-3	F13	Nail	■		■	■		■			
X146-4	F13	Nail	■		■			■	■		
X148	F13	Long pointy artefact	■		■			■			
X163-1	F13	Little iron rod	■		■			■			
X163-2	F13	Cramp?	■		■	■					Pittings
X167	F13	Iron	■		■				■		Martensite, bainite, quenched

Table 11.6. *Summary of microstructures observed during metallography. Low-C = low carbon, mid-C = mid carbon, high-C = high carbon. Filled squares confirm observations; empty squares denote a degree of uncertainty.*

The results confirm the presence of phosphoric iron, visible as phosphoric ghost structures, a common feature of iron made in western Jutland. Similarly, most of the artefacts exhibit steel parts, ranging from low- to high-carbon microstructures, with high-carbon microstructures often associated with steel produced from Norwegian iron. No clear pattern or relationship can be discerned between the archaeological phases and the types of iron microstructures observed (i.e. ferritic iron, phosphoric iron, low carbon steel, mid-carbon steel, and high-carbon steel). High-carbon steel appears to coincide with phases F7, F10, and F13, though given the nature of sampling, it would be prudent not to extrapolate further.

The metallographic results confirm the presence of steel from phase F7 onwards.

Provenancing

Slag inclusion (SI) analysis has been a popular tool for provenancing ferrous artefacts for the last twenty years, particularly in the past decade. The premise is that original slag trapped within an iron artefact can be matched to the slag by-product from bloomery iron production (the direct process). The method does not appear to work for iron made from the indirect process (i.e. cast iron from a blast furnace). Bloomery iron production slags (traditional ironmaking, also known as the bloomery process) from archaeological sites can be used as reference material by which to compare and make provenance hypotheses for iron artefacts containing analysable SI. For a long time, the main composition was deemed sufficient for determining broad provenance hypotheses (Birch & Martinón-Torres 2015; Blakelock et al. 2009; Buchwald 2005; Buchwald & Wivel 1998; Charlton et al. 2012; Dillman & L'Héritier 2007), using major oxide compounds such as soda (Na_2O), magnesia (MgO), alumina (Al_2O_3), silica (SiO_2), phosphorus (P_2O_5), sulphur (SO_3), potash (K_2O), lime (CaO), titania (TiO_2), manganese (MnO), iron (FeO), and baria (BaO). Whilst this approach remains employed and is well practiced in Denmark, it has received criticism for being imprecise at the local level. It does appear to work for provenancing at the regional level, however, especially in regard to Scandinavia and its varied geology (Buchwald & Wivel 1998; Charlton et al. 2012; Ilkjær, Jouttijärvi & Andresen 1994; Jouttijärvi 2013; Lyngstrøm 2008). Trace-element analysis of SI has been increasingly used to complement traditional analyses of major oxides to provide a more robust approach for provenancing iron (Charlton 2015; Desaulty et al. 2009a; 2009b; 2008; Leroy et al. 2012; Stepanov et al. 2020; Żabiński et al. 2020). It is not the purpose here to provide an exhaustive background of iron provenancing, but recent publications can be consulted for an extensive overview (Stepanov et al. 2020; Żabiński et al. 2020). Iron provenancing via the SI analytical method was employed using the main composition (major and minor oxides) only for exploring regional provenance hypotheses. The approach here is identical to that outlined and graphically displayed in a recent study of Iron-age iron lances from Jutland (Birch 2018).

Entrapped SI within the iron artefacts were analysed for their chemical composition using a scanning electron microscope (SEM) coupled to an energy dispersive X-ray spectrometer (EDS). A Zeiss Evo LS25 SEM-EDS system (housed at the School of Engineering, NAVITAS/Aarhus University) was used for imaging and compositional analysis. Viewing and imaging was performed in both secondary electron (SE) and backscattered-electron (BS) modes. Individual spectra were examined to identify element peaks and exported as tables of compositions using AZtec software (Oxford Instruments). Entrapped inclusions were analysed from 34 artefacts, yielding 144 compositional analyses with a mean analytical total of 99.9(±8.5) wt% (median – 101.1 wt%) prior to normalization. Three artefacts from the original 37 selected were not analysed chemically: X1319 was identified as pyrite mineral and therefore not subjected to chemical analysis, X137 could not be analysed, and X143–4 was identified as an ultra-high-carbon steel (borderline cast iron), making it ineligible for SI analysis. The full dataset of normalized compositions of inclusion analyses is provided in the appendix.

The SI compositions were first screened to separate smithing inclusions from original SI. Smithing inclusions derive from processes such as welding, fluxing, and oxidizing, normally being very rich in silica (from fluxing with sand) and/or iron oxide (oxidation of welded surfaces), and thus are not SI to the original iron. It is important to filter these inclusions out so that they do not affect the iron-provenancing analysis. The SI compositions, therefore, were first screened to separate smithing inclusions from original SI (Fig. 11.8), using Jouttijärvi's schema (2015; 2013; 2009). The remaining data was used to calculate the average (mean) SI composition for each

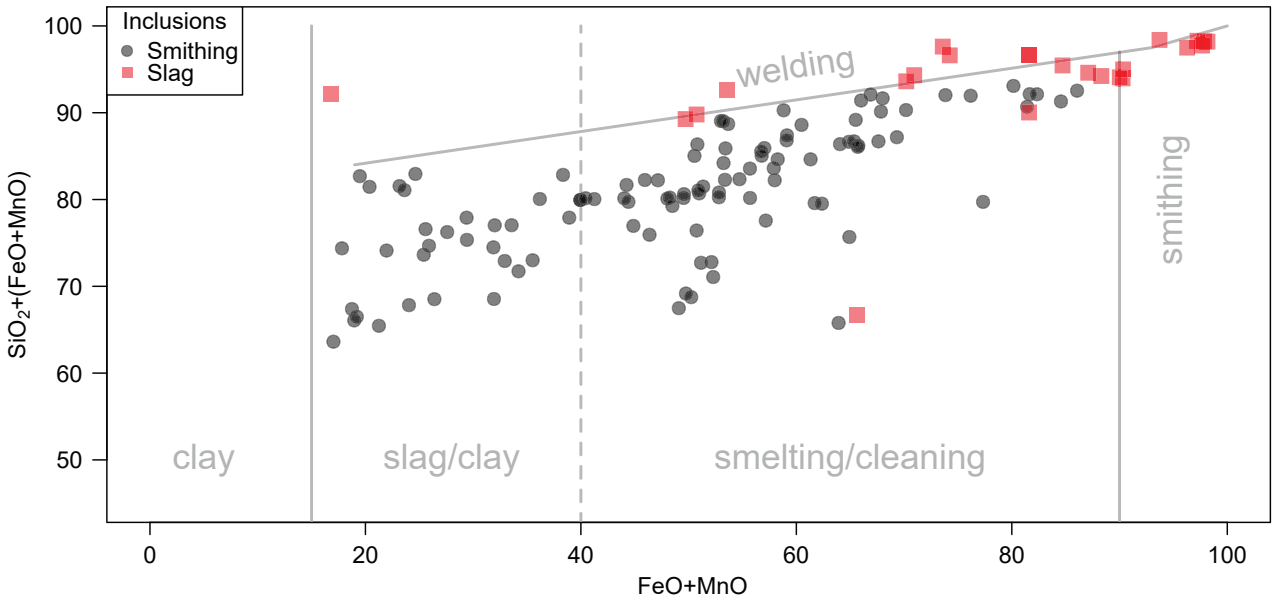

Figure 11.8. *Bivariate scatterplot of major oxides used to distinguish smithing inclusions from innate slag inclusions in iron. Schema after Jouttijärvi (2009; 2013; 2015). Two of the inclusions are visible within the smelting/cleaning zone: these are two inclusions from X1210 rich in P_2O_5, likely representing iron oxide inclusions that have become enriched in phosphorus as it oxidizes from the metal phase.*

Find no.	Phase	n=	Na_2O	MgO	Al_2O_3	SiO_2	P_2O_5	SO_2	K_2O	CaO	TiO_2	MnO	FeO
X1294	F5	5	0.6	3.5	4.2	36.9	0.4	0.4	1.4	7.2		14.2	31.3
X1036	F7	12	0.3	5.1	3.7	41.9	0.3	2.3	1.7	11.9	1.3	15.6	19.7
X1149-1	F7	1	0.0	2.7	5.7	35.5	0.1	0.6	1.2	2.5	0.8	3.2	47.7
X1149-2	F7	4	0.6	0.4	3.4	23.6	7.8	1.0	1.2	1.9	0.2	0.3	60.6
X1149-3	F7	4	0.2	1.1	7.6	34.5	4.1	0.7	2.5	2.2	0.4	0.5	46.3
X1149-4	F7	2	0.5	0.3	1.0	18.8	0.4		0.2	1.4	0.1		77.3
X1149-5	F7	4	0.4	0.9	8.9	44.0	2.0	0.5	4.1	4.8	0.4	1.1	34.5
X1149-6	F7	4	0.6	0.4	6.6	20.3	2.6	1.6	0.9	0.8	0.2	0.5	66.5
X799	F9	2	0.1	0.4	2.6	30.4	8.5	0.5	0.9	1.0		0.7	55.1
X811	F9	4	0.8	0.7	5.1	33.5	1.9	0.1	1.7	3.0	0.3	0.3	52.8
X833	F9	7	0.7	0.8	5.0	12.9	19.6	0.6	1.0	0.8		0.4	59.8
X614-1	F10	2	2.1	3.2	13.2	37.5	1.3	0.1	2.2	5.6		3.2	31.7
X614-2	F10	4	0.5	1.4	5.2	26.2	0.6	0.8	1.3	2.3	0.3	18.1	43.2
X614-3	F10	4	0.3	1.9	11.7	38.3	3.2	0.6	2.0	9.3	0.4	4.2	28.3
X614-4	F10	4	1.0	1.0	10.1	60.2	0.1	0.3	2.9	2.0	0.6	11.3	10.6
X632	F10	2	0.0	0.2	5.1	35.9	1.2	0.4	2.1	1.8	0.3	0.9	52.2
X640	F10	2	0.8	2.4	10.5	36.7	0.9	1.7	1.8	2.2		24.3	20.1
X133-1	F13	4	0.3	1.8	5.4	21.2	4.5	0.7	1.7	3.5	0.5	2.7	57.8
X133-2	F13	3	0.7	0.7	5.9	17.0	1.9	0.7	1.1	1.3	0.3	4.2	67.4
X133-3	F13	4	0.1	0.8	7.6	29.9	8.4	0.4	1.1	1.6	0.3	0.3	49.6
X143-1	F13	4	0.3	0.5	3.4	23.1	2.3	0.3	1.0	0.8	0.3	4.0	64.6
X143-2	F13	4	0.6	2.9	17.9	46.0	0.6	0.1	5.9	4.8	0.7	13.1	10.1
X143-3	F13	3	0.4	1.3	4.2	8.6	0.6	0.8	0.3	1.7	0.3	0.3	82.5
X143-5	F13	4	0.5	0.9	4.5	26.1	4.8	0.7	1.8	2.9	0.5	5.9	52.5
X146-1	F13	4	0.3	1.2	8.9	30.0	4.7	0.3	2.7	1.7	0.4	7.1	42.9
X146-2	F13	4	0.3	1.0	8.1	31.0	1.9	0.5	1.9	5.4	0.5	1.5	48.0
X146-3	F13	3	3.2	1.7	5.4	16.3	0.8	0.5	1.3	2.9	0.4	1.4	72.3
X146-4	F13	4	0.5	1.2	1.2	19.3	9.8	0.5	1.1	7.5	0.8	23.7	34.4
X148	F13	3	0.0	2.5	1.6	19.5	3.2	1.5	0.3	1.8		10.5	59.2
X163-2	F13	4	1.4	0.5	10.7	48.8	4.2	0.7	5.4	2.7		1.0	24.7

Table 11.7. *Mean SI compositions (major and minor oxides) for each artefact calculated from the normalized dataset after screening out smithing inclusions. Values expressed in wt%. n=number of analyses per artefact. Missing values = beneath detection limits.*

artefact shown in Table 11.7. Three further artefacts had to be excluded from the provenancing analysis: X1210, X846, and X167 were excluded from the provenance study because the analyses revealed only smithing inclusions. SI compositions of artefacts were subsequently compared to the relevant compositions of iron-production slags from Scandinavia that were published in Buchwald (2005, Tables 6.2, 6.4, 7.1, 7.6, 8.1–2, 8.4, 9.1, 9.3–5, 10.1, 10.5, 10.7–8, 12.8, 12.11), referred to here as the reference data used in Figs 11.9–11.

Iron ores from western Jutland are characterized by a high phosphorus content, making this a useful element for crudely distinguishing local iron from that from the Scandinavian Peninsula. A bivariate scatterplot showing P_2O_5 and CaO (Fig. 11.9) serves to highlight artefacts containing elevated phosphorus content, whilst the elevated CaO values may be related to corrosion processes. The usefulness of this plot is limited by the fact only two oxide components are displayed from a multivariate dataset.

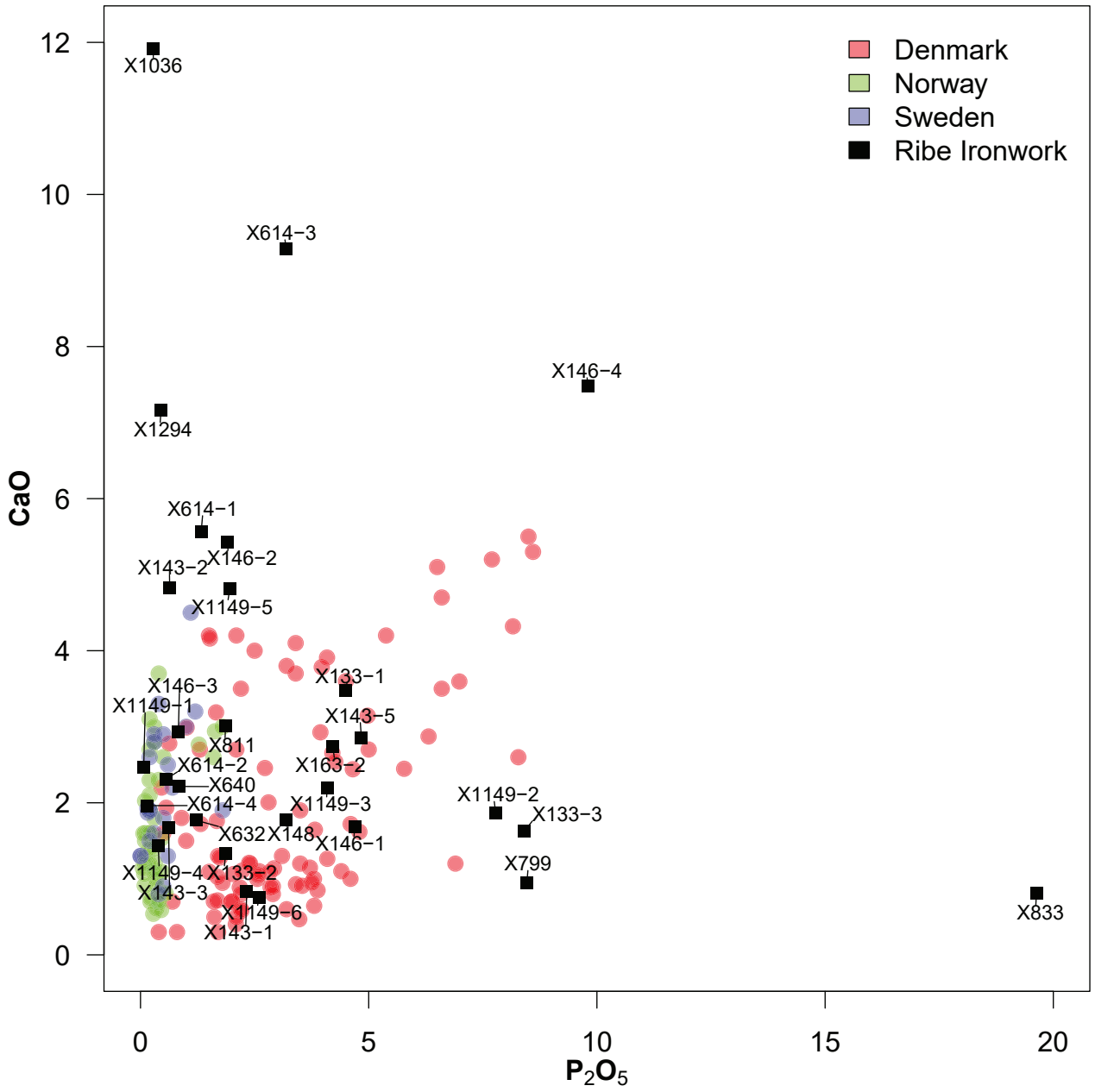

Figure 11.9. *Bivariate scatterplot of P_2O_5 and CaO comparing the iron artefacts to reference iron production data (Buchwald 2005).*

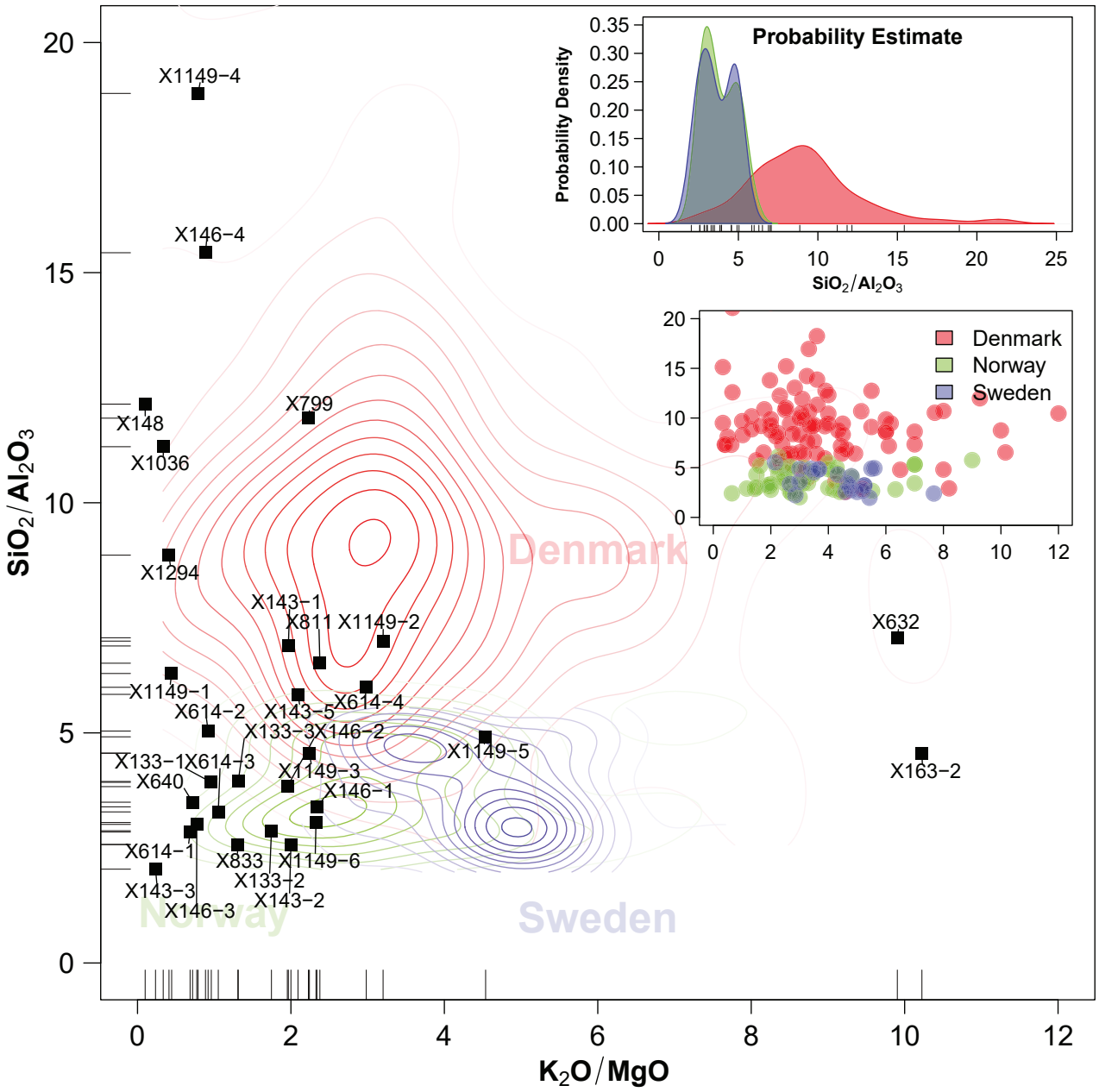

Figure 11.10. *Bivariate scatterplot of SiO_2/Al_2O_3 against K_2O/MgO with the average SI composition of SJM 3 Posthustorvet iron artefacts plotted as points and with iron production sources represented as a contour plot (raw data points shown in the embedded plot, middle right). Probability density plot of iron production regions (embedded, top right) with rug marks along the x axis (SiO_2/Al_2O_3) corresponding with iron samples; the same rug marks shown in the main plot along both axes.*

By encompassing more oxide components, more of the multivariate compositional variability can be represented in a single bivariate scatterplot, as shown in Fig. 11.10. This method, employing SiO/Al_2O_3 and K_2O/MgO ratios, has been used repeatedly to provenance iron within Scandinavia (Buchwald 2005; Buchwald & Wivel 1998). It is not without limitations but serves as a necessary and useful first step towards making hypotheses of the regional provenance of artefacts. Provenance hypotheses for the artefacts studied are provided in Table 11.8, based on an interpretation of Fig. 11.10, using the threshold value of 5 for the SiO_2/Al_2O_3 ratio to distinguish between the Scandinavian Peninsula (<5) and Jutland (>5). An attempt to further discriminate between iron-production sources was made via a robust PCA from multivariate analytical methods in compositional data analysis

Find no.	Phase	Denmark	Norway
X1294	F5	◆	
X1036	F7	◆	
X1149-1	F7	◆	
X1149-2	F7	◆	
X1149-3	F7		◆
X1149-4	F7	◆	
X1149-5	F7		◆
X1149-6	F7		◆
X799	F9	◆	
X811	F9	◆	
X833	F9		◆
X614-1	F10		◆
X614-2	F10	◆	
X614-3	F10		◆
X614-4	F10	◆	
X632	F10	◆	
X640	F10		◆
X133-1	F13		◆
X133-2	F13		◆
X133-3	F13		◆
X143-1	F13	◆	
X143-2	F13		◆
X143-3	F13		◆
X143-5	F13	◆	
X146-1	F13		◆
X146-2	F13		◆
X146-3	F13		◆
X146-4	F13	◆	
X148	F13	◆	
X163-2	F13		?

Table 11.8. *Provenance hypotheses of ironwork based on an interpretation of Fig. 11.8. Note that Norway is suggested due to other evidenced connections, but it may also represent the Scandinavian Peninsula region more widely.*

(Templ et al. 2011). The resulting PCA biplot (Fig. 11.11) provided mixed results, however; mostly they confirmed the previous identifications but also challenged some. The most likely explanation for this is the problem associated with mixing different datasets produced from different analytical setups. Future work would do well to employ trace element analyses of SI to help distinguish more clearly potential provenance sources.

Discussion

Despite issues of preservation and identification, the iron and slag remains recovered from SJM 3 Posthustorvet appear to largely conform to results from previous excavations and research. They indicate that larger/heavier slags are associated with earlier phases of settlement, probably related to bloom refining (primary smithing), whilst later phases are characterized by smaller/lighter slag fragments indicative of secondary smithing. The metallographic examination of the artefacts confirms an array of different microstructures as well as technological practices associated with the production of nails. The different types of iron alloy do not appear to correlate with chronological phases; rather, they demonstrate the presence of steel artefacts from early in the site's chronology (phase F7). An analysis of SI has revealed that iron from both Jutland and the Scandinavian Peninsula (Norway) were being used in tandem throughout successive phases. It seems that Norwegian steel was prevalent at Ribe from its initial development. What is equally interesting to observe is that Danish iron appears to have been used until phase F13, as is indicated by the finds studied. This implies that iron was still being produced in the locality, despite the real lack of evidence for iron production in Viking-age Jutland. Future studies will seek to further advance the provenance of iron artefacts with greater resolution and reliability through the application of trace-element analysis.

The primary scope of this chapter has been to investigate the iron objects, and their provenance to further the understanding of Ribe's trade and production of iron artefacts. However, a comparative study of iron from other urban Viking-age locations, such as Hedeby, Kaupang, and Birka, would greatly benefit the discussion on iron production and trade, thus furthering our knowledge on trade aspects in Viking-age towns.

Authors' contributions

Lauridsen surveyed the iron finds provided from the SJM 3 Posthustorvet excavations and made the sample selection of nails (or similar) for archaeometallurgical analysis, aided by X-radiographs. Lauridsen prepared the metallographic blocks and conducted the microscopic study of microstructures. Zolbin supervised the preparation of the metallographic specimens and conducted the chemical analysis of entrapped slag inclusions with Lauridsen, who

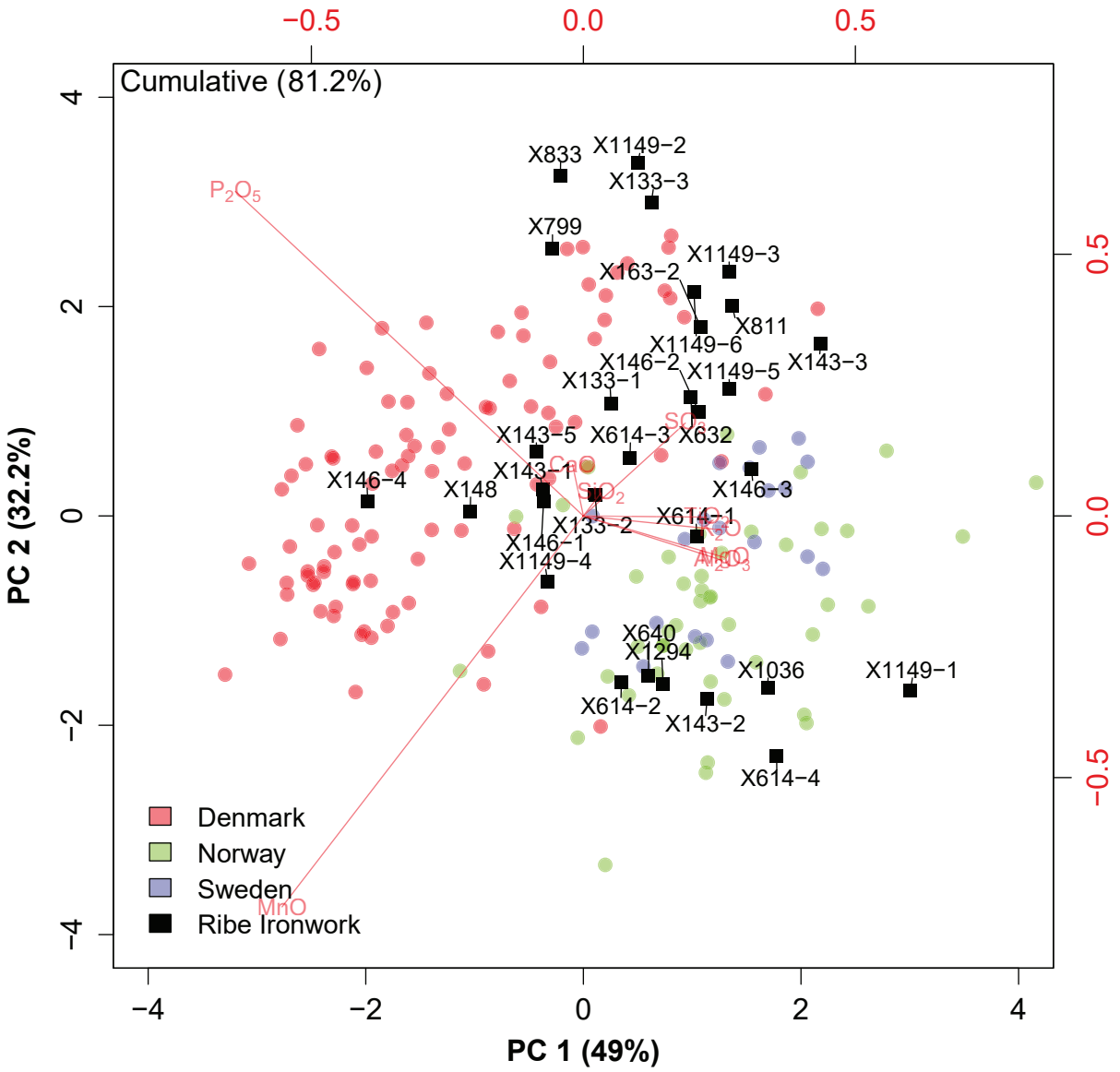

Figure 11.11. *Robust PCA biplot of the major and minor oxide components (excluding NaO and FeO) of iron production reference data and SJM 3 Posthustorvet ironwork analysed.*

then conducted a provenancing study. Lauridsen drafted the first version of the manuscript, which was revised with original contributions by Birch: namely, the chronological summary of iron remains and slag debris, the section on provenancing, and the final discussion.

Bibliography

Ashby, S.P., A.N. Coutu & S.M. Sindbæk 2015. Urban Networks and Arctic Outlands: Craft Specialists and Reindeer Antler in Viking Towns. *European Journal of Archaeology* 18, 679–704. doi:10.1179/1461957115Y.0000000003

Baug, I., D. Skre, T. Heldal & Ø.J. Jansen 2019. The Beginning of the Viking Age in the West. *Journal of Maritime Archaeology* 14, 43–80. doi:10.1007/s11457-018-9221-3

Birch, T. 2018. Standardised Manufacture of Iron Age Weaponry from Southern Scandinavia: Constructing and Provenancing the Havor Lance, in: A. Dolfini, R.J. Crellin, C. Horn & M. Uckelmann, eds. *Prehistoric Warfare and Violence: Quantitative and Qualitative Approaches*. Quantitative Methods in the Humanities and Social Sciences. Cham: Springer International Publishing, 247–276. doi:10.1007/978-3-319-78828-9_12

Birch, T. & M. Martinón-Torres 2015. The iron bars from the 'Gresham Ship': employing multivariate statistics to

further slag inclusion analysis of ferrous objects. *Historical Metallurgy* 48(2), 69–78.

Blakelock, E., M. Martinón-Torres, H.A. Veldhuijzen, & T. Young 2009. Slag inclusions in iron objects and the quest for provenance: an experiment and a case study. *Journal of Archaeological Science* 36, 1745–1757.

Buchwald, V.F. 2005. *Iron and Steel in ancient times.* Historisk-filosofiske skrifter 29. Copenhagen: The Royal Danish Academy of Sciences and Letters.

Buchwald, V.F. & O. Voss 1992. Iron production in Denmark in Viking and Medieval times, in: A. Espelund, ed. *Bloomery Ironmaking during 2000 Years, Vol. 2*. Trondheim: Budalseminaret, 31–43.

Buchwald, V.F. & H. Wivel 1998. Slag Analysis as a Method for the Characterization and Provenancing of Ancient Iron Objects. *Materials Characterization* 40, 73–96. doi:10.1016/S1044-5803(97)00105-8

Charlton, M.F. 2015. The last frontier in 'sourcing': the hopes, constraints and future for iron provenance research. *Journal of Archaeological Science* 56, 210–220. doi:10.1016/j.jas.2015.02.017

Charlton, M.F., E. Blakelock, M. Martinón-Torres & T. Young 2012. Investigating the production provenance of iron artifacts with multivariate methods. *Journal of Archaeological Science* 39, 2280–2293. doi:10.1016/j.jas.2012.02.037

Desaulty, A.-M., C. Mariet, P. Dillmann, J.L. Joron & P. Fluzin 2008. A provenance study of iron archaeological artefacts by Inductively Coupled Plasma-Mass Spectrometry multi-elemental analysis. *Spectrochimica Acta Part B: Atomic Spectroscopy* 63, 1253–1262. doi:10.1016/j.sab.2008.08.017

Desaulty, A.-M., P. Dillmann, M. L'Héritier, B. Gratuze, J.-L. Joron & P. Fluzin 2009a. Does it come from the Pays de Bray? Examination of an origin hypothesis for the ferrous reinforcements used in French medieval churches using major and trace element analyses. *Journal of Archaeological Science* 36, 2445–2462.

Desaulty, A.-M., C. Mariet, P. Dillmann, J.L. Joron, B. Gratuze, C.M.-L. Carlier & P. Fluzin 2009b. Trace elements behaviour in direct-and indirect-iron metallurgy: The case of Pays de Bray (France). In: P. Craddock, A. Giumlia-Mair & A. Hauptman, eds. *Archaeometallurgy in Europe: 2nd International Conference 17–21 June 2007, Aquileia, Italy: Selected Papers.* Milan: Associazione Italiana di Metalurgia, 318–334.

Dillman, P. & M. L'Héritier 2007. Slag inclusion analyses for studying ferrous alloys employed in French medieval buildings: supply of materials and diffusion of smelting processes. *Journal of Archaeological Science* 34, 1810–1823. doi:10.1016/j.jas.2006.12.022

Ilkjær, J., A. Jouttijärvi & J. Andresen 1994. *Illerup Ådal: Proveniensbestemmelse af jern fra Illerup ådal – et pilotprojekt.* Moesgård: Jysk Arkæologisk Selskab.

Jouttijärvi, A. 2009. The Shadow in the Smithy. *Materials and Manufacturing Processes* 24, 975–980. doi:10.1080/10426910902987176

Jouttijärvi, A. 2013. Iron and processes in Scandinavian blacksmithing workshops from the Iron Age to the 14th century. In: J. Humphris & T. Rehren, eds. *The World of Iron.* London: Archetype Publications, 402–408.

Jouttijärvi, A. 2015. Scales and spheres. *Historical Metallurgy* 48, 41–46.

Leroy, S., S.X. Cohen, C. Verna, B. Gratuze, F. Téreygeol, P. Fluzin, L. Bertrand & P. Dillmann 2012. The medieval iron market in Ariège (France). Multidisciplinary analytical approach and multivariate analyses. *Journal of Archaeological Science* 39, 1080–1093. doi:10.1016/j.jas.2011.11.025

Lyngstrøm, H. 2008. *Dansk Jern: En kulturhistorisk analyse af fremstilling, fordeling og forbrug.* København: Det kongelige nordiske Oldskriftselskab.

Madsen, H.B. 2004. Smithing Debris. In: M. Bencard, A.K. Rasmussen & H.B. Madsen, eds. *Ribe Excavations 1970–76, Vol. 5*. Esbjerg: Jutland Archaeological Society, 187–222.

Ottaway, P. 2004. Ribe Ironworks. In: M. Bencard, A.K. Rasmussen & H.B. Madsen, eds. *Ribe Excavations 1970–76, Vol. 5*. Esbjerg: Jutland Archaeological Society, 103–172.

Rundberget, B. 2015. Sørskandinavisk jernutvinning i vikingetiden – lokal produksjon eller handelsprodukt? In: A. Pedersen & S.M. Sindbæk, eds. Et fælles hav: Kattegat og Skagerrak i Vikingetiden: seminar på Nationalmuseet, København, 19.–20. september 2012, København: Nordlige Verdener, Nationalmuseet, 168–187.

Stepanov, I.S., L. Weeks, K.A. Franke, B. Overlaet, O. Alard, C.M. Cable, Y.Y. Al Aali, M. Boraik, H. Zein & P. Grave 2020. The provenance of early Iron Age ferrous remains from southeastern Arabia. *Journal of Archaeological Science* 120. doi:10.1016/j.jas.2020.105192

Templ, M., K. Hron & P. Filzmoser 2011. robCompositions: An R-package for Robust Statistical Analysis of Compositional Data. In: V. Pawlowsky-Glahn & A. Buccianti, eds. *Compositional Data Analysis: Theory and Applications*. Chichester: Wiley, 341–355.

Żabiński, G., J. Gramacki, A. Gramacki, E. Miśta-Jakubowska, T. Birch & A. Disser 2020. Multi-classifier majority voting analyses in provenance studies on iron artefacts. *Journal of Archaeological* Science 113. doi:10.1016/j.jas.2019.105055

Appendix

Normalized SI compositions from SEM-EDS analyses of iron artefacts. Results are normalized and presented as element oxides in weight percent (wt %). Analyses deemed to be smithing inclusions are asterisked (*) after the Finds no. anal.=Analysis. Blank values represent elements beneath detection limits. Note that analyses for X1210, X846, and X167 consist entirely of smithing inclusions.

Find no.	Note	Phase	Anal.	Na_2O	MgO	Al_2O_3	SiO_2	P_2O_5	SO_2	K_2O	CaO	TiO_2	MnO	FeO
X1294		F5	1		5.31	0.85	31.46		0.26	0.23	3.08		15.18	43.64
X1294		F5	2	0.68	2.88	4.98	36.31	0.68	0.39	1.60	6.54		12.86	33.08
X1294		F5	3	1.31	1.02	6.98	42.61	0.05	0.66	2.53	12.97		10.90	20.98
X1294		F5	4	0.05	2.53	4.84	39.71	1.01	0.50	1.91	9.00		14.00	26.44
X1294		F5	5	0.52	5.78	3.18	34.49	0.05	0.32	0.92	4.20		18.10	32.44
X1210*		F6	1	0.11	0.21	0.19		32.33		0.07			0.70	66.40
X1210*		F6	2		0.20	2.75	1.07	29.00	0.79	0.37	0.15		0.71	64.95
X1210*		F6	3	0.12		0.42	2.68	2.45	0.14	0.09	0.01			94.08
X1210*		F6	4	0.08	0.13	0.54	3.68	4.73	0.17	0.10	0.28		0.06	90.22
X1210*		F6	5	0.07		0.14	4.06	5.32	0.03	0.05	0.31		0.17	89.85
X1210*		F6	6	0.30	0.05	0.78	10.55	12.40	0.29	0.14		0.28		75.20
X1210*		F6	7	0.07	0.23	0.80	8.43	8.48		0.30	0.10		0.04	81.56
X1036	centre	F7	1	0.37	3.27	2.51	28.90	0.65	0.36	0.98	5.94		9.15	47.88
X1036	centre	F7	2	0.44	4.32	3.07	40.00		1.02	1.66	9.56		17.65	22.30
X1036	centre	F7	3			0.19	2.40	0.49	17.77		1.82		0.85	76.48
X1036	centre	F7	4		5.75	3.77	52.44		0.81	2.36	11.70		23.17	
X1036	centre	F7	5	0.14	5.27	4.03	43.87	0.06		1.49	8.96		16.68	19.51
X1036	centre	F7	6	0.44	4.32	3.07	40.00		1.02	1.66	9.56		17.65	22.30
X1036*	centre (weld line?)	F7	7			52.58	46.78		0.36				0.27	
X1036	second part	F7	8	0.21	5.34	5.39	56.56	0.37		2.70	11.61		13.64	4.18
X1036	third part	F7	1	0.24	5.87	4.53	48.63		0.29	2.16	18.17	1.34	15.12	3.63
X1036	third part	F7	2	0.23	4.27	5.52	46.59		0.36	1.41	22.91	1.68	12.40	4.63
X1036	third part	F7	3		5.55	5.00	44.20	0.10	0.24	1.44	21.24	1.00	15.20	6.05
X1036	third part	F7	4	0.31	5.99	3.89	51.01	0.24	0.53	1.26	11.18		23.08	2.50
X1036	third part	F7	5	0.20	5.76	3.88	48.52	0.05	0.34	1.54	10.32		22.64	6.75
X1149-1*		F7	1	0.44	0.88	1.59	23.39	0.44	0.14	0.49	1.68		0.17	70.77
X1149-1		F7	2	0.04	2.74	5.65	35.54	0.07	0.64	1.22	2.47	0.82	3.15	47.66
X1149-1*		F7	3		0.51	1.40	10.74	0.18	0.91	0.35	0.77	0.42	1.26	83.45
X1149-2		F7	1		0.34	3.23	20.45	6.01	1.38	0.74	1.97	0.13	0.49	65.26
X1149-2		F7	2	0.75	0.46	3.26	26.36	6.95		1.96	1.98		0.06	58.21
X1149-2		F7	3		0.08	3.47	23.31	7.77	0.71	1.14	1.93	0.25	0.22	61.10
X1149-2		F7	4	0.52	0.66	3.53	24.23	10.40		1.09	1.59		0.25	57.74
X1149-3		F7	1	0.03	1.14	7.37	30.14	4.38	0.88	2.54	1.83	0.33	0.39	50.96
X1149-3		F7	2	0.19	1.37	7.57	35.07	3.37	0.40	3.16	1.50	0.22	0.43	46.72
X1149-3		F7	3	0.47	0.71	7.62	37.44	3.81	0.81	1.82	2.77	0.31	0.50	43.74
X1149-3		F7	4	0.29	1.18	7.69	35.32	4.79	0.59	2.34	2.66	0.74	0.49	43.92
X1149-4*		F7	1	0.23	0.37	0.82	15.06	0.37	0.02	0.28	1.17	0.08	0.22	81.37
X1149-4*		F7	2	0.23	0.37	0.82	15.06	0.37	0.02	0.28	1.17	0.08	0.22	81.37
X1149-4		F7	3	0.40	0.22	1.04	20.52	0.11		0.16	1.58	0.03		75.94
X1149-4		F7	4	0.51	0.35	0.95	17.08	0.67		0.29	1.29	0.19		78.68
X1149-5		F7	1	0.21	0.85	8.37	36.11	2.36	0.53	3.45	3.96	0.12	0.52	43.51
X1149-5		F7	2	0.52	0.98	9.18	43.47	2.38		4.12	5.11	0.66	1.29	32.28
X1149-5		F7	3	0.38	0.65	7.57	38.80	1.74		4.58	4.69	0.36	1.08	40.17
X1149-5		F7	4		1.09	10.66	57.46	1.34			5.49	0.35	1.69	21.93
X1149-6		F7	1	1.10	0.03	13.12	31.97	1.47		2.16	1.54	0.36	0.63	47.62
X1149-6		F7	2	0.30	0.80	4.52	6.48	0.70		0.60	0.23	0.31	0.19	85.87
X1149-6		F7	3	0.40	0.48	5.83	20.37	4.70	1.44	0.20	0.82	0.06	0.72	64.98

Find no.	Note	Phase	Anal.	Na_2O	MgO	Al_2O_3	SiO_2	P_2O_5	SO_2	K_2O	CaO	TiO_2	MnO	FeO
X1149-6		F7	4	0.45	0.16	3.10	22.28	3.51	1.71	0.46	0.41	0.08	0.41	67.44
X799		F9	1		0.48	2.21	25.70	11.18	0.77	0.79	0.98		0.69	57.21
X799		F9	2	0.12	0.31	2.92	35.03	5.75	0.31	0.97	0.92		0.67	53.00
X811		F9	1	0.58	0.66	5.17	32.47	2.58		1.87	2.96	0.29	0.10	53.32
X811		F9	2	0.85	0.41	4.04	28.89	2.27	0.09	1.60	2.14	0.06		59.64
X811		F9	3	1.00	0.78	4.66	28.12	1.09	0.13	1.07	2.43	0.24	0.39	60.09
X811		F9	4	0.71	0.96	6.70	44.50	1.52	0.19	2.14	4.52	0.42	0.38	37.96
X833		F9	1	1.01	1.05	5.54	18.51	20.93	0.71	1.14	0.86		0.10	50.14
X833		F9	2				2.35	6.82						90.83
X833		F9	3	1.09		6.16	19.42	21.44		1.16	0.99		0.46	49.29
X833		F9	4		0.68	2.74	10.76	19.61	0.44	0.53	0.33		0.51	64.41
X833		F9	5	0.72	0.69	5.01	18.39	23.43	1.19	1.09	0.38		1.13	47.96
X833		F9	6	0.48	0.90	6.03	1.86	24.12	0.19	1.12	1.39		0.10	63.82
X833		F9	7	0.43	0.61	4.51	18.79	21.06	0.26	1.13	0.94		0.31	51.97
X846*		F9	1	0.03			24.03	1.09		0.57	0.25	0.44	0.11	73.48
X846*		F9	2		0.23	1.70	22.37	0.60	0.29	0.27		0.31	0.13	74.11
X846*		F9	3	0.33	0.29	0.55	5.92	3.39	0.56	0.24		0.40	0.07	88.24
X846*		F9	4		0.50	0.89	4.66	2.97		0.38	0.19	0.08	0.01	90.32
X614-1		F10	1	1.68	3.88	12.99	37.48	1.14		1.77	5.55		2.69	32.83
X614-1		F10	2	2.49	2.57	13.36	37.52	1.52	0.10	2.65	5.58		3.69	30.52
X614-2		F10	1	0.58	2.24	5.08	28.26	0.61	0.47	1.20	2.17	0.27	19.12	40.01
X614-2		F10	2	0.67	0.76	4.47	20.13	0.39	0.92	0.84	1.56	0.09	13.59	56.59
X614-2		F10	3	0.41	1.11	4.81	27.72	0.64	1.19	1.79	2.85	0.38	20.64	38.46
X614-2		F10	4	0.52	1.53	6.46	28.80	0.61	0.81	1.36	2.67	0.49	19.03	37.71
X614-3		F10	1	0.37	1.49	8.30	29.57	4.41	0.61	1.87	6.97	0.06	4.28	42.09
X614-3		F10	2	0.26	1.65	11.99	36.61	6.58		2.34	8.03	0.60	4.44	27.49
X614-3		F10	3	0.27	2.36	12.34	39.99	0.74		1.77	9.32	0.28	3.23	29.70
X614-3		F10	4	0.31	2.25	14.06	47.11	1.04	0.55	2.18	12.83	0.72	4.95	14.01
X614-4		F10	1	0.98	1.06	10.03	61.08		0.51	3.03	2.60	0.33	14.20	6.18
X614-4		F10	2	0.90	1.24	10.26	58.38	0.14	0.17	2.88	2.04	0.82	13.62	9.55
X614-4		F10	3	1.23	0.74	9.94	63.21		0.31	3.00	1.66	0.44	8.96	10.52
X614-4		F10	4	0.81	0.87	10.00	58.31		0.36	2.75	1.55	0.71	8.42	16.22
X632		F10	1		0.21	5.25	36.05	1.16	0.37	1.95	1.66	0.34	0.79	52.21
X632		F10	2	0.01		4.92	35.82	1.28	0.47	2.21	1.88	0.20	1.01	52.20
X632*		F10	3				1.05	0.39	0.84	0.07	0.41		0.53	96.71
X632*		F10	4	0.24	0.02	0.65	0.03	0.17	0.41	0.02	0.23	0.08	0.25	97.91
X640		F10	1	1.28	3.09	13.19	45.03	0.85		2.16	2.40		22.56	9.44
X640*		F10	2			0.57	1.22	0.30	1.63				1.23	95.05
X640		F10	3	0.25	1.80	7.79	28.27		1.73	1.35	2.03		25.95	30.83
X133-1		F13	1	0.34	1.77	6.70	20.67	8.54	1.16	2.89	5.23	0.59	2.91	49.21
X133-1		F13	2	0.50	1.89	4.85	24.48	6.02	0.92	2.22	2.87	0.55	3.11	52.59
X133-1		F13	3	0.03	1.52	5.56	21.76	1.48	0.32	0.93	3.07	0.43	2.08	62.81
X133-1		F13	4	0.25	1.91	4.48	17.85	1.94	0.33	0.78	2.73	0.41	2.88	66.45
X133-2		F13	1	0.52	0.48	4.35	10.48	0.88	0.48	0.35	0.81		3.72	77.94
X133-2		F13	2		0.78	4.24	12.94	0.99			0.66	0.25	2.35	77.80
X133-2		F13	3	0.84	0.69	9.11	27.45	3.73	0.92	1.92	2.52		6.39	46.42
X133-3		F13	1	0.03	1.43	6.87	28.90	5.97	0.74	1.27	1.35	0.07	0.27	53.10
X133-3		F13	2	0.19	0.57	8.06	30.77	8.74	0.05	1.09	1.66	0.38	0.33	48.16
X133-3		F13	3	0.04	0.87	7.63	27.98	7.70	0.40	0.89	1.59	0.08	0.52	52.30
X133-3		F13	4	0.10	0.45	7.80	32.09	11.21		1.11	1.90	0.48	0.09	44.78
X143-1		F13	1			3.64	25.20	2.52	0.44		1.14	0.16	4.41	62.48
X143-1		F13	2		0.51	3.64	25.40	2.30	0.32	1.09	0.73		4.98	61.03
X143-1		F13	3	0.34	0.50	3.22	23.65	2.42		0.92	0.75	0.19	3.35	64.66
X143-1		F13	4	0.18	0.47	2.92	18.19	2.07	0.17	0.90	0.73	0.52	3.45	70.39
X143-2		F13	1	0.78	3.01	18.30	47.29		0.11	5.47	4.90	0.93	12.32	6.88
X143-2		F13	2	0.82	2.72	17.08	43.79	0.71	0.03	5.45	4.41	0.96	14.03	10.01
X143-2		F13	3	0.58	3.35	19.89	50.83		0.14	6.49	5.11	0.34	13.27	

Find no.	Note	Phase	Anal.	Na_2O	MgO	Al_2O_3	SiO_2	P_2O_5	SO_2	K_2O	CaO	TiO_2	MnO	FeO
X143-2		F13	4	0.32	2.65	16.24	42.12	0.57	0.15	6.05	4.87	0.63	12.94	13.46
X143-3		F13	1	0.44	1.54	3.78	9.26	0.82		0.22	2.09	0.42	0.33	81.09
X143-3		F13	2	0.64	1.32	3.10	9.79			0.37	2.23	0.21	0.01	82.33
X143-3		F13	3	0.04	0.91	5.77	6.74	0.41	0.84		0.71		0.41	84.15
X143-5		F13	1		0.59	3.72	21.34	4.40	0.91	1.18	2.05	0.44	3.68	61.68
X143-5		F13	2	0.21	0.29	3.41	22.33	4.79	0.69	1.69	2.05	0.49	5.00	59.05
X143-5		F13	3	0.72	1.18	5.37	29.73	4.95	0.48	2.59	3.53	0.47	7.29	43.69
X143-5		F13	4		1.42	5.38	30.96	5.22			3.78		7.51	45.73
X146-1		F13	1	0.41	1.46	11.00	38.99	3.23		3.54	2.35	0.11	8.35	30.57
X146-1		F13	2	0.22	1.05	7.34	25.69	10.45	0.43	2.25	1.28	0.55	5.83	44.91
X146-1		F13	3	0.13	1.40	8.34	27.62	2.59	0.34	2.72	1.72	0.41	7.07	47.65
X146-1		F13	4		0.79	8.73	27.87	2.52	0.02	2.48	1.38	0.52	7.31	48.38
X146-2		F13	1	0.05	0.72	8.54	30.65	1.96	0.18	2.02	5.81	0.55	1.38	48.15
X146-2		F13	2	0.39	0.87	7.92	30.14	1.43	0.84	0.41	6.04	1.06	1.32	49.59
X146-2		F13	3	0.42	1.14	8.61	32.08	2.53		2.58	4.33	0.29	1.48	46.55
X146-2		F13	4	0.50	1.10	7.27	31.05	1.73	0.51	2.47	5.53	0.27	1.95	47.62
X146-3		F13	1	1.44	0.97	10.62	48.66	1.50	0.83	1.89	5.78	0.73	1.40	26.19
X146-3		F13	2	4.97	2.50	0.23	0.30	0.16	0.17	0.79	0.08	0.12		90.69
X146-3		F13	3				0.05							99.95
X146-4		F13	1	0.91	1.00	1.26	20.41	8.47	0.33	1.64	7.71	1.11	22.32	34.84
X146-4		F13	2	0.44	1.24	1.39	17.15	7.65	0.56	1.25	7.19	0.75	24.23	38.14
X146-4		F13	3	0.09	1.05	1.14	17.89	10.31	0.63	1.16	5.80	0.21	25.36	36.34
X146-4		F13	4	0.46	1.63	1.20	21.56	12.81	0.64	0.31	9.22	1.03	22.99	28.16
X148*		F13	1		0.57	2.63	7.52		1.37	0.01	0.80		2.41	84.68
X148		F13	2		2.73	0.67	23.67	4.70	0.10		2.62		9.81	55.70
X148		F13	3	0.04	1.00	2.53	15.78	0.52	1.51	0.18	2.25		7.16	69.02
X148		F13	4		3.80	1.62	19.08	4.35	2.74	0.32	0.47		14.65	52.97
X148*		F13	5		1.18	2.82	23.42	1.34	0.27	0.06	0.72		14.01	56.19
X163-1*		F13	1		0.95	0.80	0.08	0.14		0.02		0.35	1.95	95.71
X163-1*		F13	2	0.23	0.44	0.86	0.38	0.11		0.06	0.06		2.13	95.74
X163-2		F13	1	1.75	0.21	11.93	52.16	3.82	0.76	5.04	2.36		0.78	21.18
X163-2		F13	2	1.47	0.59	9.86	45.93	5.09	1.06	4.44	2.14		1.73	27.69
X163-2		F13	3	1.58	0.59	10.87	48.23	3.89		5.76	3.68		1.01	24.40
X163-2		F13	4	0.91	0.74	10.15	48.77	4.06	0.17	6.54	2.77		0.43	25.47
X167*		F13	1		0.51			0.03	0.69		0.08		0.30	98.39
X167*		F13	2	0.23	0.19		4.68	0.24	0.58	0.05	0.32		0.86	92.85
X167*		F13	3	0.29	0.81	2.32	39.06	0.36	2.97	0.66	2.50	0.30	6.22	44.52
X167*		F13	4	0.53	0.52	2.75	39.55	0.81	2.83	0.72	2.52	0.07	6.15	43.57
X167*		F13	5	0.56	0.41	3.35	75.40		0.33	1.60	1.54		3.48	13.33
X167*		F13	6	0.67	1.03	2.74	39.11	0.12	0.09	0.53	1.96	0.22	3.38	50.15

Catalogue of metallography results

This catalogue reports the examination of specimens using a metallurgical reflected-light microscope (Zeiss AX10, Observer A1m with magnifying 100x/0.8 HD, housed at the School of Engineering, NAVITAS/Aarhus University). Images of the microstructures observed were recorded as optical micrographs using the Zen software. The results are summarized with detailed descriptions of individua samples. The catalogue can be accessed online at: XXXXX